AGES OF STELLAR POPULATIONS IN THE LOW-METALLICITY STAR-FORMING DWARF GALAXIES

N. G. Guseva

Main Astronomical Observatory, NAS of Ukraine
27 Akademika Zabolotnoho Str., 03680 Kyiv, Ukraine
e-mail: guseva@mao.kiev.ua

We perform a comprehensive study of ten star-forming (SF) galaxies with the oxygen abundance $Z < Z_{\odot}/20$ [5] and blue extended low-surface-brightness components (LSB). Long-slit spectroscopy and V, I CCD photometry were obtained with the Kitt Peak 2.1-m and 4-m telescopes, the 4.5-m MMT, the 2.4-m HST and the 10-m Keck II telescopes. We use two extinction-insensitive methods based on the equivalent widths of (1) emission and (2) absorption Balmer lines to put constraints on the age of the stellar populations (SP). In addition, we use two extinction-dependent methods based on (3) the spectral energy distribution and (4) the $(V-I)$ colour. Several scenarios of star formation were explored using all four methods. We compare the photometric and spectroscopic properties of the ten low-metallicity SF galaxies with those of a sample of 16 well-known dwarf irregular and blue compact dwarf (BCD) galaxies. We show that there is a clear trend for the stellar LSB component of lower-metallicity galaxies to be bluer. However, the observed trend is too steep to be explained only by metallicity effects. Therefore, the lower-metallicity galaxies have also younger populations. In particular, the luminosity-weighted ages of galaxies with LSB colours of $(V-I) < 0.6$ are not greater than 1–2 Gyr. Our finding is confirmed by analysing of high-redshift galaxies and the fossil record of the SPs of nearby galaxies: the stellar birthrate for most massive galaxies peaked at z > 1 (or $\sim$10 Gyr) just as for low-mass galaxies efficient star formation have been triggered at z ~ 0.2 (or ~ 2 Gyr).

INTRODUCTION

Blue compact dwarf (BCD) galaxies are characterized by the ongoing intense star formation (SF) activity as evidenced by strong nebular emission lines superposed on a blue continuum (*e.g.*, [16, 18]). They are compact and metal-deficient objects with the oxygen abundance ranging between 1/50 and 1/3 of the solar one [5] (*e.g.*, [15]) and possess large amounts of neutral gas. Low metal abundances place these objects among the least chemically evolved galaxies in the universe.

Sargent & Searle [18] proposed that the BCD galaxies are actually experiencing their first burst of star formation. However, most of the BCDs studied so far have the revealed extended low surface brightness red stellar sheets underlying the blue star-forming regions. Some of these stellar sheets have been resolved with the *Hubble Space Telescope* (*HST*) into red giant stars. This indicates the presence of evolved low-mass stellar populations in the underlying host galaxies.

The tiny fraction of galaxies with an extremely low oxygen abundance in the ionized gas (less than 1/20 $(\mathrm{O/H})_{\odot}$) has been suggested by Izotov & Thuan [15] to be young galaxies, based on chemical element abundance arguments. Nearly about ten such galaxies with good abundance determinations are known to date. During several last years we performed a comprehensive study of the ten star-forming (SF) galaxies with oxygen abundances $Z < Z_{\odot}/20$ and blue extended low-surface-brightness components. The outer parts of these galaxies are unusually blue. The spectral energy distributions and colours of their outskirts are consistent with those of stellar populations which have ages less than a few 100 Myr (see the examples of SBS 0335–052 [11, 13] and I Zw 18 [12]).

Despite the compiling the new large samples of emission-line galaxies, such as Sloan Digital Sky Survey (SDSS), Two-Degree Field Galaxy Redshift Survey (2dF GRS), up to now metal-poor galaxies with the oxygen abundance $Z < Z_{\odot}/20$ are very rare in the local universe. The proximity of these metal-poor galaxies allows to study their structure, metal content, and stellar populations with the sensitivity, precision, and spatial resolution that the faint, small angular size, distant high-redshift galaxies do not allow. Detailed spectroscopic and photometric studies of extremely metal-poor BCDs based on observations with large telescopes are useful to

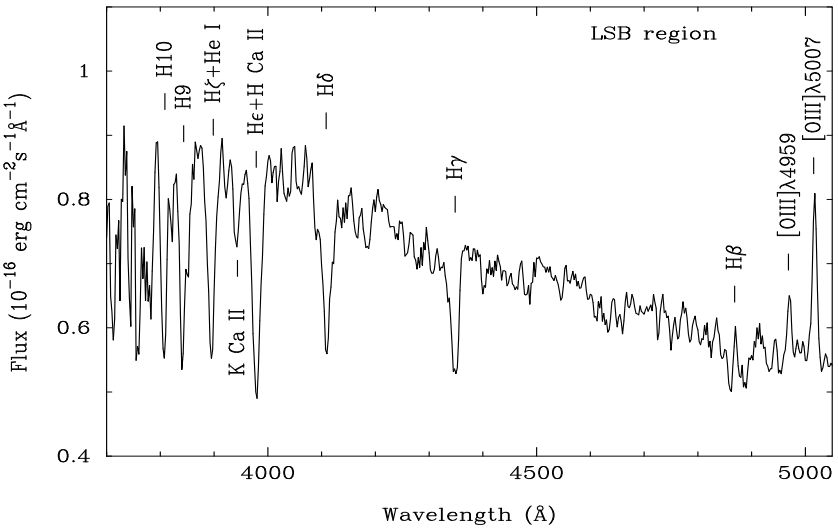

Figure 1. The spectrum of a low-surface-brightness region with labeled emission and absorption lines

shed light on the origin of these galaxies, deduce their star formation history, constrain their ages and compare with high-redshift galaxies.

AGE OF THE STELLAR POPULATION IN THE LSB REGIONS

Long-slit spectroscopy and V, I CCD photometry for ten local most metal-poor galaxies were obtained with the Kitt Peak 2.1-m and 4-m telescopes, the 4.5-m Multiple Mirror Telescope (MMT), the 10-m Keck II telescope and the 2.4-m *Hubble Space Telescope* (*HST*). The spectra of the brightest regions in the galaxies show strong emission lines and blue continua dominated by a very young stellar population of resent burst of star formation with the age not more than several Myrs. The old stellar populations if present are masked by a bright emission from the H II region. Focusing on the evolutionary status of the galaxies, especially on the age of the oldest stars contributing to the light of the galaxies, we study the properties of the stellar population in an extended low surface brightness component. Figure 1 shows the observed spectrum of one of the BCDs with hydrogen emission and absorption lines of the LSB region.

METHODS

We use four various methods, three of which are based on the use of spectroscopic data and the fourth one – on the use of photometric data. Two of these methods use the time evolution of equivalent widths of the hydrogen Balmer emission and absorption lines which are detected in almost all regions along the slit. The other two methods are based on the comparison of observed and theoretical spectral energy distributions (SED) and broad-band colours. All the aforementioned methods are sensitive to the star formation history. The first two methods are extinction-insensitive, while the others depend on both the properties of the stellar population and the interstellar extinction. Several scenarios of star formation were explored for all four methods. An instantaneous burst model is most appropriate for the brightest H II star-forming regions in a galaxy. To obtain the upper limit on the age of the stellar population in the LSB regions we adopt a continuous SF scenario with constant or variable star formation rates (SFRs). The use of all four methods allows us to put constraints on the star formation history and properties of the stellar population as well as to estimate the interstellar extinction. These methods are described in detail in [6–9].

For the first method we consider two limiting cases of instantaneous burst and continuous star formation models. The instantaneous burst model equivalent widths of H_α and H_β emission lines are calculated using the galactic evolution code PEGASE.2 [3] for various heavy element mass fractions. PEGASE.2 is based on the Padua stellar evolutionary models [1] and stellar atmosphere models from Lejeune *et al.* [17]. An initial mass function with a Salpeter slope ($\alpha = -2.35$), and upper and lower mass limits of 120 $M_\odot$ and 0.1 $M_\odot$ are adopted for all our calculations with the PEGASE.2 code. In continuous star formation models we adopt a constant star formation rate in the interval between the time t_i when star formation starts and t_f when it stops. Time is equal to zero now and increases to the past. We use the modelled equivalent widths of the hydrogen emission lines and

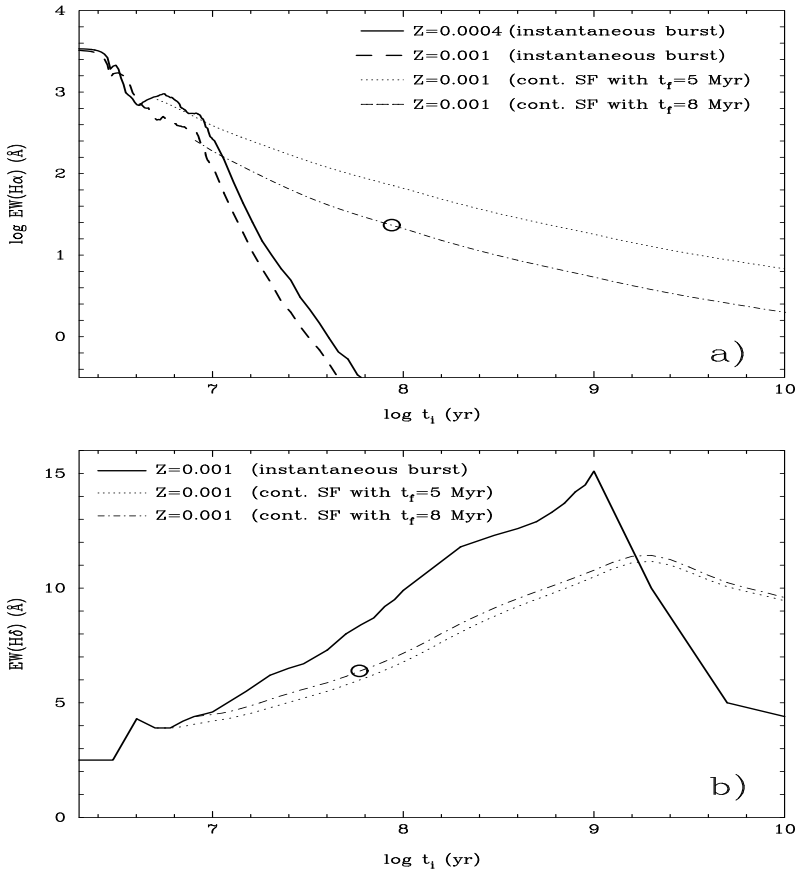

Figure 2. (a) Time evolution of the equivalent width (EW) of the nebular emission line H_α for an instantaneous burst with the heavy element mass fraction $Z = Z_\odot/20$ (dashed line) and $Z = Z_\odot/50$ (solid line). Model predictions are also shown for the case of a constant continuous star formation starting at an age defined by the abscissa t_i and stopping at t_f, with $t_f = 5$ Myr (dotted line) and $t_f = 8$ Myr (dash-dotted line), both with $Z = Z_\odot/20$. Circle shows the position of the observed LSB region with the observed EW (H_α) superposed on the modelled curve for the continuous star formation stopping at $t_f = 8$ Myr. (b) Dependence of the equivalent width of the H_δ absorption line for an instantaneous burst on age for ages > 1 Gyr from [2] and for ages ≤ 1 Gyr with the metallicity $Z{=}Z_\odot/20$ from [4] is shown by solid line. Model predictions are also shown for the case of a constant continuous star formation starting at an age defined by the abscissa t_i and stopping at t_f, with $t_f = 5$ Myr (dotted line) and $t_f = 8$ Myr (dash-dotted line), both with $Z = Z_\odot/20$. Circle shows the position of the observed LSB region with the corrected EW (H_δ) superposed on the models of the continuous star formation with $t_f = 8$ Myr

SEDs for instantaneous bursts [3] to calculate the temporal evolution of the equivalent width of the hydrogen emission lines in the case of a continuous star formation with the constant SFR. The temporal dependence of the equivalent width of the H_α emission line is shown in Fig. 2a.

In the second method we use the relation between the H_δ and H_γ absorption line equivalent widths and age, which are derived from models developed by González Delgado, Leitherer & Heckman [4]. In addition, we use an empirical calibration of the hydrogen absorption line equivalent width versus age by Bica & Alloin [2]. This calibration is based on integrated spectra of 63 open and globular stellar clusters with well known ages, metallicities and reddenings which can be used as templates for stellar populations formed in an instantaneous burst. The temporal evolution of the H_γ and H_δ absorption line equivalent widths in the case of continuous SF is calculated similarly to that of the H_α and H_β emission line equivalent widths for the first method. The temporal evolution of the H_δ absorption line equivalent width is shown in Fig. 2b.

The shape of the spectrum (3rd method) reflects the properties of a stellar population. However, it is also dependent on the reddening. Therefore, the observed SED cannot directly give information on the age, but should be used together with the first and second methods for the simultaneous determination of the age and interstellar extinction. We used the galactic evolution code PEGASE.2 to produce a grid of theoretical SEDs for

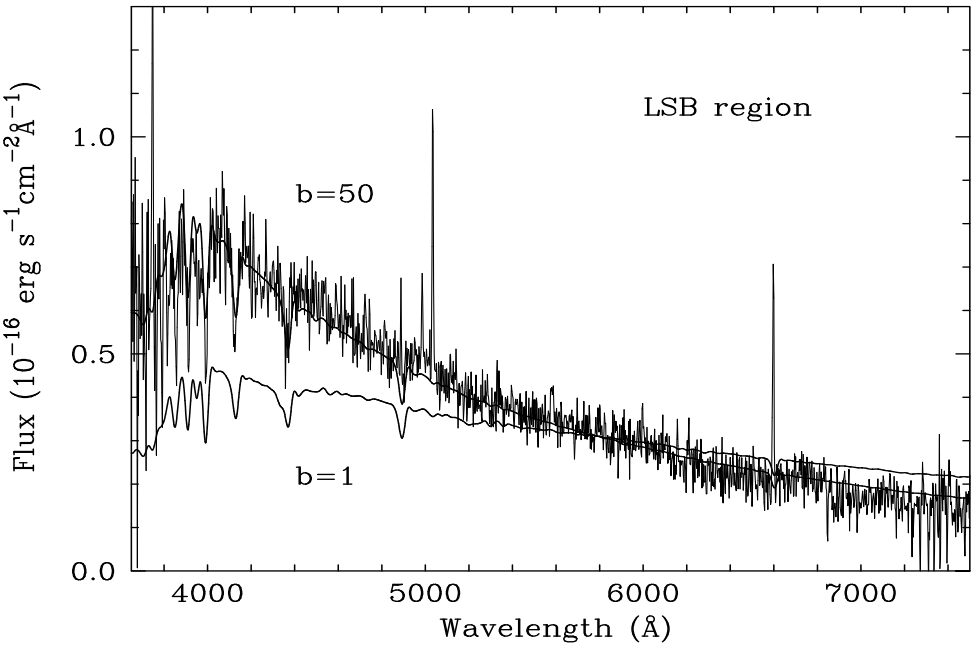

Figure 3. Spectrum of a LSB region on which synthetic continuum spectral energy distributions are superposed. Synthetic SED labeled by $b \equiv$ SFR($t \leq 100$ Myr)/SFR($t > 100$ Myr) = 1 corresponds to a stellar population forming continuously with a constant star formation rate since 10 Gyr ago. Synthetic spectrum labeled by $b = 50$ corresponds to a stellar population forming continuously between 0 and 10 Gyr with a star formation rate enhanced by a factor of b during the last 100 Myr. These SEDs are superposed on the observed spectrum uncorrected for extinction. The spectrum uncorrected for extinction gives the upper limit of the age of the stellar population

an instantaneous burst of star formation with ages ranging between 0 and 10 Gyr, and different heavy element mass fractions. The SEDs for continuous SF in the time interval between $t_{\rm i}$ ago and $t_{\rm f}$ ago are derived by the integration of instantaneous burst SEDs. We consider several SF histories and vary extinction in the LSB regions to put constraints on the age of their stellar populations. Synthetic SEDs are calculated for stellar populations forming continuously during one or two time intervals with different durations of the time intervals. In the case of two intervals the SFR varies from one interval to another one by a factor b = SFR(young)/SFR(old). Figure 3 shows the spectra of an LSB region on which the synthetic SEDs with two different SF histories are superposed. An upper limit to the age of the LSB region can be obtained by assuming no extinction, *i.e.*, $C(\rm H_\beta) = 0$.

In the fourth method we derived the V and I surface brightness and colour distributions for the bright and LSB regions covered by spectroscopic observations at slit orientations and compared them with predictions from our population synthesis modelling (Fig. 4). The observed $(V - I)$ colour of the brightest H II regions are usually very blue ($\sim$ –0.5) (Fig. 4b), and cannot be reproduced by a stellar population of any age. This is because of a large contribution of very strong oxygen and hydrogen emission lines, as evidenced by their large equivalent widths, and gaseous continuum. However, in outer LSB regions the equivalent widths of the emission lines are small. Therefore, for those regions we will not take into account an ionized gas emission.

RESULTS

Our spectroscopic analysis of the LSB regions using three methods favours a relatively young luminosity-weighted age of the stars populating those regions. All the spectroscopic properties of the LSB regions can be explained by only young and intermediate-age stellar populations with the age not more than 1–2 Gyr.

We also compared the observed colours with predictions from our population synthesis modelling (fourth method). The example of this comparison is shown in Fig. 4. The predicted colours, obtained from convolving the theoretical SEDs with the appropriate filter bandpasses, are shown by different symbols for various star formation histories. The agreement between the $(V - I)$ colours and those derived from the spectral energy distributions is very good.

Our comprehensive studies of ten selected galaxies with the oxygen abundances 12 + log(O/H) < 7.6 and blue LSB components have led us to the conclusion that these galaxies might be young. This is in contrast to

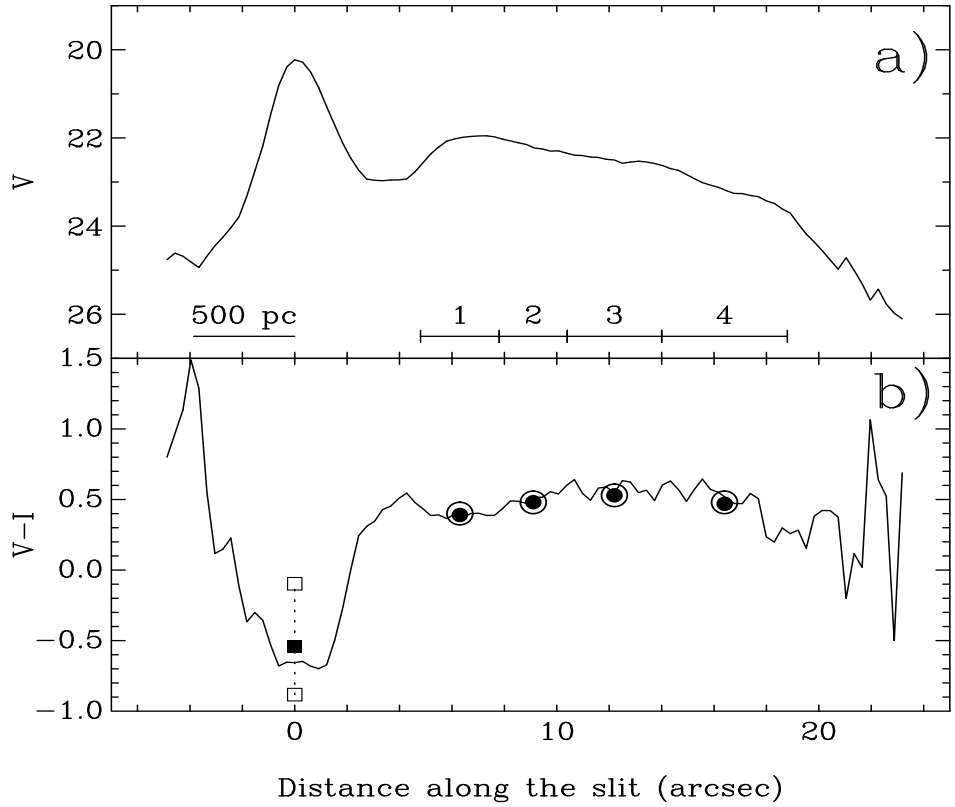

Figure 4. (a) The V surface brightness distribution along the slit in one of the BCDs. The origin is at the location of the brightest H II region. The regions used for spectroscopic analysis are labeled in (a) from "1" to "4". (b) The $V-I$ colour distribution along the slit. Filled circles are the predicted colours of a stellar population continuously formed with a constant star formation rate between 8 Myr and 100 Myr ago and reddened with an extinction coefficient as derived for each region. Open circles are the predicted colours of the stellar populations continuously formed between 0 and 10 Gyr with the enhancement parameters b as derived for each region from 3rd method. The filled square indicates the colour of a 4 Myr stellar population to which the observed ionized gas emission in the brightest H II region has been added. The upper open square shows the colour of a pure 4 Myr stellar population, while the lower open square shows the colour of a pure ionized gas emission

a large age estimated for some well-studied higher-metallicity irregular and BCD galaxies, such as VII Zw 403 and UGCA 290. To investigate this apparent inconsistency we therefore compare the (V–I) colours of the LSB components ($(V–I)_{LSB}$) of the galaxies from our sample with those in galaxies where a large age was derived from colour-magnitude diagrams (CMD).

The dependence of the $(V–I)_{LSB}$ colours on oxygen abundance for 26 selected galaxies (ten galaxies from our sample and 16 ones from a comparison sample) is shown in Fig. 5. Thin dashed lines represent theoretical dependences for an instantaneous burst in the age range from $\log t_{\rm i} = 7.1$ to $\log t_{\rm i} = 10.0$ ($t_{\rm i}$ in yr). The models of a continuous star formation are shown by thick solid lines. These models are calculated for a constant SFR which has started at time $t_{\rm i}$ with $\log t_{\rm i}$ between 7.5 and 10.0 and is continuing until now ($t_{\rm f} = 0$). We see a clear trend in colours for the stellar LSB component of lower-metallicity galaxies. The LSB components in the low-metallicity galaxies are systematically more blue. However, the observed trend is too steep to be explained only by metallicity effects (see theoretical curves in Fig. 5, solid and dashed lines). Therefore, the lower-metallicity galaxies have also younger populations. In particular, the luminosity-weighted ages of galaxies with LSB colours of $(V-I) < 0.6$ mag are not greater than 1–2 Gyr.

Our finding is confirmed by analysing of high-redshift galaxies and the fossil record of the stellar populations of the nearby galaxies: Heavens *et al.* [10] indicate a very different formation history for high- and low-mass galaxies, the stellar birthrate for most massive galaxies peaked at redshift z $>$ 1 (or $\sim$ 10 Gyr) just as for low-mass galaxies an efficient star formation have been triggered at z $\sim$ 0.2 (or $\sim$ 2 Gyr).

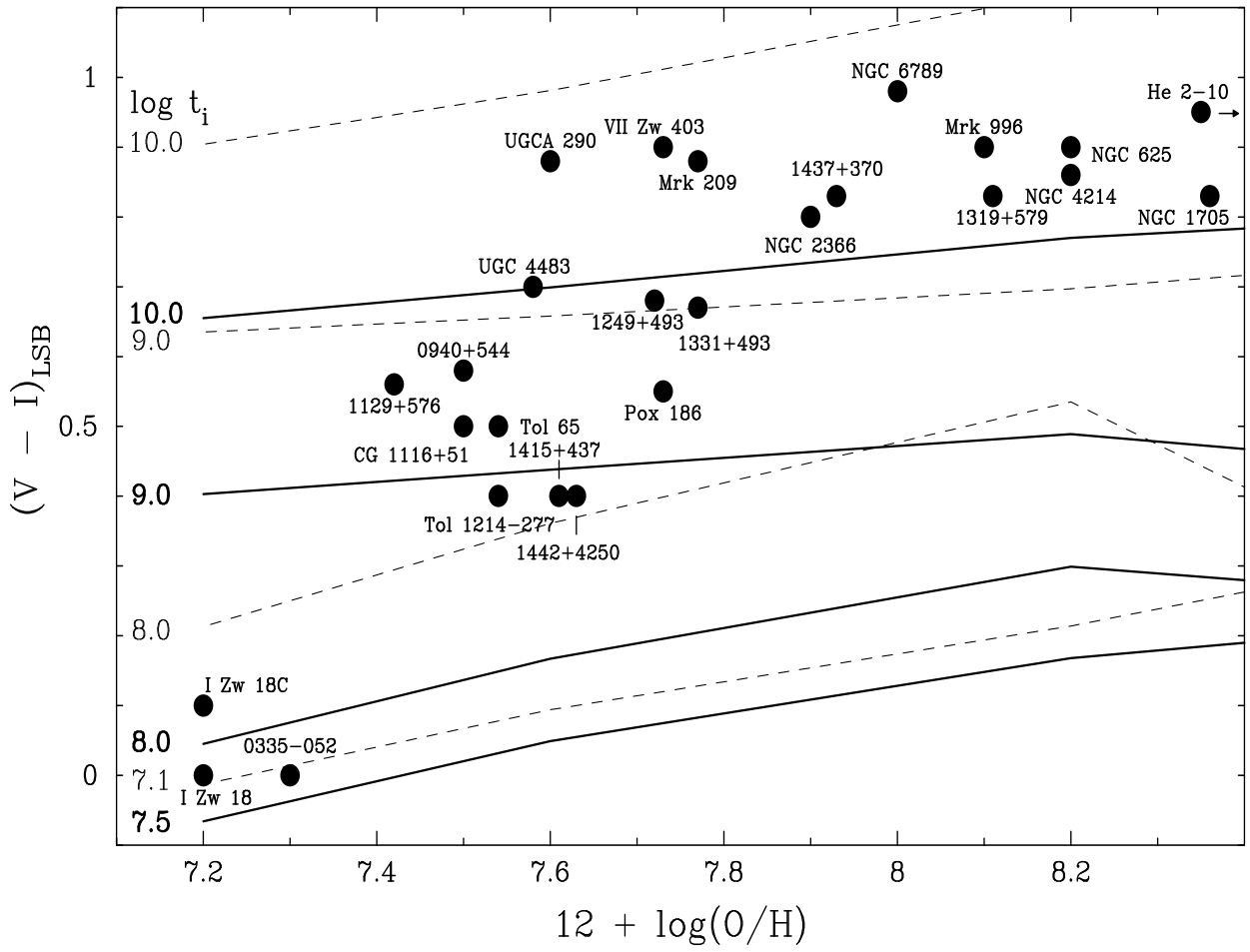

Figure 5. Dependence of the $(V-I)$ colours of the LSB component on the oxygen abundance for the galaxies from our sample with the oxygen abundance 12 + log(O/H) < 7.6 and from a comparison sample with higher metallicity. Dashed lines show theoretical dependences of the $(V–I)$ colour on the oxygen abundance for an instantaneous burst calculated using the galactic evolution code PEGASE.2 [3] in the range of ages (in logarithmic scale) log $t_{\rm i}$ between 7.1 and 10.0 ($t_{\rm i}$ in yr). Solid lines show models in which stars are forming continuously with a constant SFR between $t_{\rm f}=0$ and various $t_{\rm i}$, where log $t_{\rm i}$ varies between 7.5 and 10.0. The observed colours are corrected only for reddening in our Galaxy

A deep photometric study of the I Zw 18 galaxy in V and I band up to 29 mag performed recently by Izotov & Thuan [14] also confirms our finding. The analysis of the colour-magnitude diagram based on the data from the *Hubble Space Telescope* Advanced Camera for Surveys revealed that the red giant branch stars are absent and that the young main sequence stars have a radial distribution on the disc of the galaxy which is more extended than the asymptotic giant branch stars. This means that the oldest stars in the galaxy are not older than 0.5 Gyr and I Zw 18 is a bona fide young galaxy.

[1] *Bertelli G., Bressan A., Chiosi C., et al.* Theoretical isochrones from models with new radiative opacities // Astron. and Astrophys. Suppl. Ser.–1994.–**106**, N 1.–P. 275–302.

[2] *Bica E., Alloin D.* A grid of star cluster properties for stellar population synthesis // Astron. and Astrophys. Suppl. Ser.–1986.–**66**, N 2.–P. 171–179.

[3] *Fioc M., Rocca-Volmerange B.* PEGASE: a UV to NIR spectral evolution model of galaxies. Application to the calibration of bright galaxy counts // Astron. and Astrophys.–1997.–**326**, N 2.–P. 950–962.

[4] *González Delgado R. M., Leitherer C., Heckman T. M.* Synthetic spectra of H Balmer and He I absorption lines. II. Evolutionary synthesis models for starburst and poststarburst galaxies // Astrophys. J. Suppl. Ser.–1999.–**125**, N 2.–P. 489–509.

[5] *Grevesse N., Noels A.* Standard abundances // Cosmic abundances: ASP Conf. Ser., 1996 / Eds S. S. Holt and G. Sonneborn.–1991.–**99**–P. 117–126.

[6] *Guseva N. G., Izotov Y. I., Papaderos P., et al.* The evolutionary status of the low-metallicity blue compact dwarf galaxy SBS 0940+544 // Astron. and Astrophys.–2001.–**378**, N 2.–P. 756–776.

[7] *Guseva N. G., Papaderos P., Izotov Y. I., et al.* Spectroscopic and photometric studies of the low-metallicity star-forming dwarf galaxies. I. SBS 1129+576 // Astron. and Astrophys.–2003.–**407**, N 1.–P. 75–90.

[8] *Guseva N. G., Papaderos P., Izotov Y. I., et al.* Spectroscopic and photometric studies of the low-metallicity star-forming dwarf galaxies. II. HS 1442+4250 // Astron. and Astrophys.–2003.–**407**, N 1.–P. 91–104.

[9] *Guseva N. G., Papaderos P., Izotov Y. I., et al.* Spectroscopic and photometric studies of the low-metallicity star-forming dwarf galaxies. III. SBS 1415+437 // Astron. and Astrophys.–2003.–**407**, N 1.–P. 105–120.

[10] *Heavens A., Panter B., Jimenez R., Dunlop J.* The star-formation history of the Universe from the stellar populations of nearby galaxies // Nature.–2004.–**428**.–P. 625–628.

[11] *Izotov Y. I., Chaffee F. H., Foltz C. B., et al.* Helium abundance in the most metal-deficient blue compact galaxies: I Zw 18 and SBS 0335–052 // Astrophys. J.–1999.–**527**, N 2.–P. 757–777.

[12] *Izotov Y. I., Chaffee F. H., Foltz C. B., et al.* A spectroscopic study of component C and the extended emission around I Zw 18 // Astrophys. J.–2001.–**560**, N 1.–P. 222–235.

[13] *Izotov Y. I., Lipovetsky V. A., Chaffee F. H., et al.* SBS 0335–052, A Probable Nearby Young Dwarf Galaxy: Evidence Pro and Con // Astrophys. J.–1997.–**476**, N 2.–P. 698–711.

[14] *Izotov Y. I., Thuan T. X.* Deep Hubble Space Telescope/ACS Observations of I Zw 18: a Young Galaxy in Formation // [`astro-ph/0408391`].–2004.

[15] *Izotov Y. I., Thuan T. X.* Heavy-element abundances in blue compact galaxies // Astrophys. J.–1999.–**511**, N 2.–P. 639–659.

[16] *Izotov Y. I., Thuan T. X., Lipovetsky V. A.* The primordial helium abundance from a new sample of metal-deficient blue compact galaxies // Astrophys. J.–1994.–**435**, N 2.–P. 647–659.

[17] *Lejeune T., Cuisinier F., Buser R.* Standard stellar library for evolutionary synthesis. II. M dwarf extension // Astron. and Astrophys. Suppl. Ser.–1998.–**130**, N 1.–P. 65–75.

[18] *Sargent W. L. W., Searle L.* Isolated Extragalactic H II Regions // Astrophys. J.–1970.–**162**, N 1.–P. L155–L159.